2818 Microsc. Microanal. 28 (Suppl 1), 2022
doi:10.1017/S1431927622010625

Failure Analysis of Conformal Cooling Inserts Fabricated by Additive Manufacturing

H. Flores-Ruiz[1, *] and R. Pérez-Bustamante[2]

[1.] Centro de Tecnología Avanzada (CIATEQ), Querétaro, Qro., México
[2.] CONACYT-Corporación Mexicana de Investigación en Materiales (COMIMSA), San Luis Potosí, SLP, México.
* Corresponding author: hiram.flores.ruiz@gmail.com

The 3D design and direct metal laser sintering (DMLS) fabrication of complex cooling circuits is rapidly gaining popularity in the injection molding industry as a powerful tool that exceeds the production capacity of conventional manufacturing with a controlled scale and cost reduction. Additive manufacturing is used to create cooling inserts known as conformal cooling inserts [1,2]. The objective of these inserts is to control and direct the solidification in a way that prevents, casting defect generation associated to shrinkages, porosities and laminations. These defects derived from solidification behavior and are linked to the lack of feeding and the natural contraction in the part. In the particular case of high pressure die casting (HPDC) it is very complex and even impossible to feed fresh material to the contraction areas [2]. Therefore, it is commonly sought to carry out a rapid and severe solidification in the problem area. An alternative solution to this problem is the implementation of conformal cooling inserts to eliminate hot spots in the feeding material (aluminum). However, the number of parts produced by the insert or shot life performance as function of manufacturing costs is critical to evaluate their permanent implementation in molds used in HPDC process.

In this work, were analyzed two different conformal cooling inserts fabricated by additive manufacturing in Maraging® steel. The inserts were provided by different suppliers and employed in a 3500 ton HPDC machine. The respective study was carried out after failure of the inserts, which occur after 4000 (insert A) and 8000 (insert B) shots respectively. Scanning electron microscopy (SEM) observations were performed on four and five zones on the fracture area of each insert respectively. Microstructural observations by optical microscopy from the fracture sections were carried out. The mechanical behavior of the samples was evaluated tensile test at room temperature and Charpy tests at three different temperatures.

Microstructural and mechanical results of insert A are presented in Fig. 1. Analyzes were carried out around the fracture of the insert. A different chemical composition is observed in each analyzed zone. An aluminum and oxygen rich-zone is presented in zone A, due to the exposition of the aluminum casted to the oxygen through the fracture. A high concentration of oxygen is also observed in zones B and D respectively, due to the corrosion of the alloying elements of the Maraging steel. On the other hand, insert B, shown in Fig. 2, present a low-concentration of aluminum near to the fracture as observed in the chemical analysis, however higher present of oxygen is observed in the areas surrounding the fracture (zones C and D), which analyses were carried out in the closer areas to the fracture.

It is observed the presence of small ruffles corresponding to each point where the laser hit the material during the additive process. An evident and considerable number of porosities generated during the additive manufacturing process is also presented. This defect can considerably affect the mechanical properties and even generate stress concentration points. On the other hand, the porous distribution on insert B is lower that the observed in insert A and the fracture can be observed in the surrounding to the conformal cooling channel. The microstructure does not present the typical additive manufacturing mark [3.4], which suggest a subsequent heat treatment carried out in the insert B after its additive fabrication. The different in microstructures and well as the difference in the mechanical behavior of the inserts observed in Figs 1a and b, are directly related with the mechanical performance of the inserts under working conditions, allowing an increment in the life service of insert B of 4000 shots in the parts production in comparison with insert A.

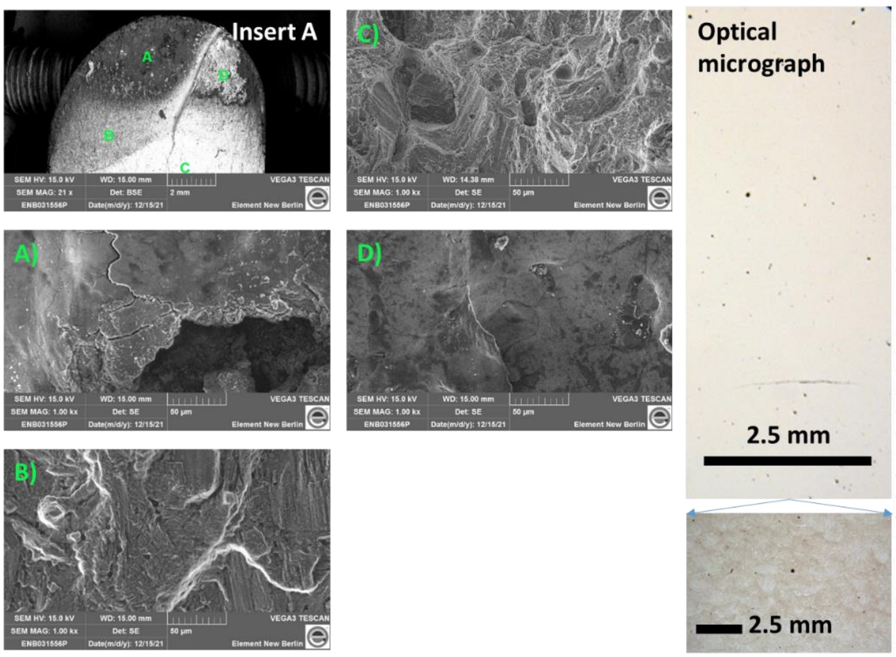

Insert A				
Element	Zone A	Zone B	Zone C	Zone D
O K	38.89	19.62	1.14	20.96
AlK	34.46	2.61	0.16	12.65
C K	8.79	14.5	2.72	5.14
FeK	5.75	42.98	66.21	37.24
SiK	4.88	1.81	0.1	2.83
CaK	2.39	1.36	0	1.67
MgK	1.44	1.48	0	2.12
CuL	1.36	0	0	0
NiK	0.9	7.39	15.36	8.98
P K	0.46	0.8	0	0.44
CoK	0.46	4.53	8.35	4.23
ClK	0.22	0.52	0	0
MoL	0	1.99	3.55	2.39
TiK	0	0.42	1.88	0.47
CrK	0	0	0.51	0
CuK	0	0	0	0.88

Tensile test	Insert A (4000 Shots)
Diameter, (in)	0.252
Original area, (in²)	0.0499
Gage length, (in)	1
Tensile strength, (psi)	214000
Yield strength, 0.2% offset, (psi)	188000
Elongation, (%)	9.5
Reduction in area, (%)	26

Specimen No.	Test temperature (°F)	Insert A (4000 Shots) Energy, (ft-lbf)
1	68	9
2	180	10
3	300	11

Figure 1. Microstructural and mechanical results of insert A

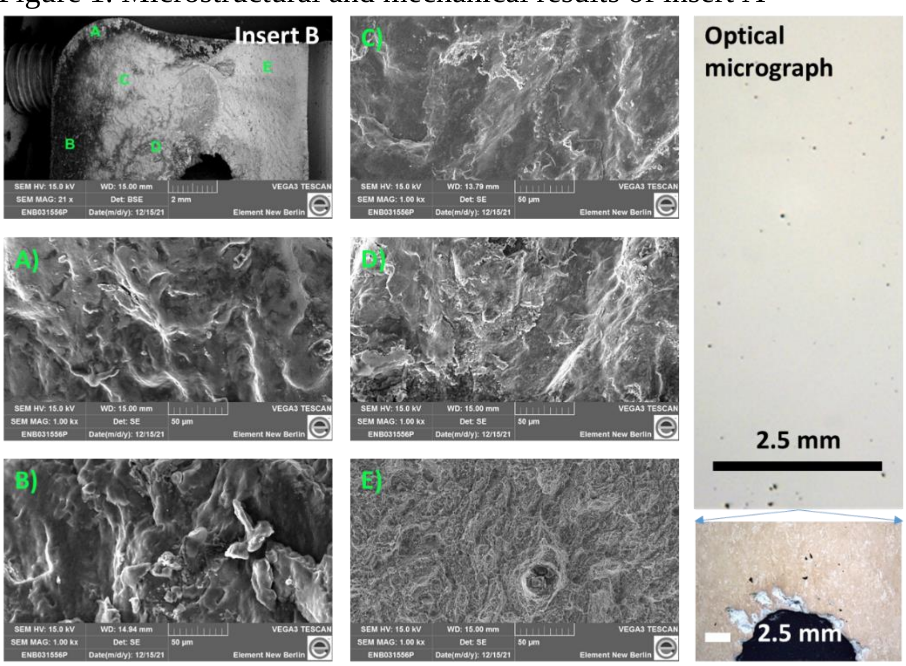

Insert B					
Element	Zone A	Zone B	Zone C	Zone D	Zone E
O K	19.12	29.62	21.45	25.65	0.94
AlK	8.88	8.17	0	1.16	0.07
C K	14.57	33.56	4.7	8.67	2.55
FeK	31.31	11.43	54.7	45.2	69.01
SiK	3.2	4.81	0.88	1.24	0
CaK	1.14	3.63	0.5	2.4	0
MgK	3.55	3.82	0	0.38	0
NiK	9.77	2.01	10.57	8.81	15.18
P K	0.2	1.06	0	0.34	0
CoK	4.76	1.12	6.57	5.22	8.19
ClK	0	0.32	0	0	0
MoL	2.45	0	0.62	0.93	2.96
TiK	0.43	0	0	0	0.97

Tensile test	Insert B (8000 Shots)
Diameter, (in)	0.251
Original area, (in²)	0.0495
Gage length, (in)	1
Tensile strength, (psi)	300000
Yield strength, 0.2% offset, (psi)	292000
Elongation, (%)	5
Reduction in area, (%)	22

Specimen No.	Test temperature (°F)	Insert B (8000 Shots) Energy, (ft-lbf)
1	68	7
2	180	7
3	300	7

https://doi.org/10.1017/S1431927622010625 Published online by Cambridge University Press

Figure 2. Microstructural and mechanical results of insert B

References

[1] K. Prantheesh, et al, Mater. Today 46 (2021), p. 7907. doi.org/10.1016/j.matpr.2021.02.567
[2] Ch. Tan, et al, Mater. Des. 196 (2020), p. 109147. doi.org/10.1016/j.matdes.2020.109147
[3] F. Fiorentini, et al, Procedia Struct. Integrity 24 (2019), p. 596. doi.org/10.1016/j.prostr.2020.02.050
[4] Z. Mao, et al, Mater. Sci. Eng., A 830 (2022), p. 142334. doi.org/10.1016/j.msea.2021.142334

https://doi.org/10.1017/S1431927622010625 Published online by Cambridge University Press